Article

TRANSPARENT PROCESS OPEN ACCESS

THE EMBO JOURNAL

Regulation of cargo-selective endocytosis by dynamin 2 GTPase-activating protein girdin

Liang Weng[1], Atsushi Enomoto[1,*], Hiroshi Miyoshi[2], Kiyofumi Takahashi[3], Naoya Asai[1], Nobuhiro Morone[4], Ping Jiang[5], Jian An[6], Takuya Kato[1], Keisuke Kuroda[7], Takashi Watanabe[7], Masato Asai[1], Maki Ishida-Takagishi[1], Yoshiki Murakumo[8], Hideki Nakashima[2], Kozo Kaibuchi[7] & Masahide Takahashi[1,**]

Abstract

In clathrin-mediated endocytosis (CME), specificity and selectivity for cargoes are thought to be tightly regulated by cargo-specific adaptors for distinct cellular functions. Here, we show that the actin-binding protein girdin is a regulator of cargo-selective CME. Girdin interacts with dynamin 2, a GTPase that excises endocytic vesicles from the plasma membrane, and functions as its GTPase-activating protein. Interestingly, girdin depletion leads to the defect in clathrin-coated pit formation in the center of cells. Also, we find that girdin differentially interacts with some cargoes, which competitively prevents girdin from interacting with dynamin 2 and confers the cargo selectivity for CME. Therefore, girdin regulates transferrin and E-cadherin endocytosis in the center of cells and their subsequent polarized intracellular localization, but has no effect on integrin and epidermal growth factor receptor endocytosis that occurs at the cell periphery. Our results reveal that girdin regulates selective CME via a mechanism involving dynamin 2, but not by operating as a cargo-specific adaptor.

Keywords clathrin-mediated endocytosis; dynamin; girdin; GTPase-activating protein; selective endocytosis

Subject Categories Cell Adhesion, Polarity & Cytoskeleton; Membrane & Intracellular Transport

DOI 10.15252/embj.201488289 | Received 20 February 2014 | Revised 28 June 2014 | Accepted 1 July 2014 | Published online 24 July 2014

The EMBO Journal (2014) 33: 2098–2112

Introduction

Eukaryotic cells utilize clathrin-mediated endocytosis (CME) to internalize various cargoes (e.g. receptors, nutrients) in a well-organized manner. This process can be dissected into five stages: nucleation, cargo selection, clathrin coat assembly, vesicle scission, and clathrin uncoating (McMahon & Boucrot, 2011). CME determines various cellular behaviors and biological properties (Doherty & McMahon, 2009), such as cell signaling pathways, migration, and polarity.

Due to the vital role of CME in cells and the diversity of cargoes that are internalized via CME, there is no doubt that the specificity and selectivity for cargoes and their timing and spacing must be precisely controlled to maintain cell homeostasis. Previous studies have demonstrated that cargo specificity is determined by the recognition of different cargoes by cargo-specific adaptors at the cargo selection stage (Traub, 2009). For example, the major clathrin adaptor, the heterotetrametric complex AP-2 (also termed adaptin), controls the endocytosis of many cargoes such as transferrin (Tf). However, ablation of AP-2 has only limited effects on low-density lipoprotein endocytosis, which is controlled by two other adaptors, disabled-2 and autosomal recessive hypercholesterolemia protein (ARH) (Keyel *et al*, 2006). Other examples of cargo-specific adaptors include epsin, β-arrestin, and numb, which are responsible for epidermal growth factor receptor (EGFR), G protein-coupled receptors (GPCR), and integrin β1 endocytosis, respectively (Huang *et al*, 2007; Nishimura & Kaibuchi, 2007; Marchese *et al*, 2008). However, even cargo-specific adaptors cannot discriminate every cargo (e.g. β-arrestin is involved in the internalization of many GPCRs, and numb regulates both integrin β1 and E-cadherin endocytosis) (Nishimura & Kaibuchi, 2007; Marchese *et al*, 2008; Sato *et al*, 2011). Given the limited number of known adaptor proteins and the variety of cargoes that are selectively internalized, additional mechanism(s) that govern selective CME remain to be identified.

During the process of endocytosis, the large GTPase dynamin plays a critical role in endocytic membrane fission events through assembling into helical polymers at the necks of budding vesicles

1 Department of Pathology, Nagoya University Graduate School of Medicine, Showa-ku, Nagoya, Japan
2 Department of Microbiology, St. Marianna University School of Medicine, Miyamae, Kawasaki, Japan
3 Department of Neuropsychiatry, St. Marianna University School of Medicine, Miyamae, Kawasaki, Japan
4 Institute for Integrated Cell-Material Sciences, Kyoto University, Sakyo-ku, Kyoto, Japan
5 The Key Laboratory of Geriatrics, Beijing Hospital and Beijing Institute of Geriatrics, Ministry of Health, Dong Dan, Beijing, China
6 Department of Respiratory Medicine, Xiangya Hospital, Central South University, Kaifu District, Changsha, China
7 Department of Cell Pharmacology, Nagoya University Graduate School of Medicine, Showa-ku, Nagoya, Japan
8 Department of Pathology, Kitasato University School of Medicine, Minami-ku, Sagamihara, Japan
*Corresponding author. Tel: +81 52 744 2093; E-mail: enomoto@iar.nagoya-u.ac.jp
**Corresponding author. Tel: +81 52 744 2093; Fax: +81 52 744 2098; E-mail: mtakaha@med.nagoya-u.ac.jp

(Ferguson & De Camilli, 2012). As a GTPase, the function of dynamin is largely dependent on binding to nucleotide and its transition from the GTP-bound form to the GDP-bound form. This process requires the involvement of GTPase-activating protein (GAP). Unlike small GTPases such as the Rho family of proteins, the activities of which are regulated by many intermolecular GAPs, dynamin GTPase activity is primarily controlled by self-assembly and its intramolecular GAP domain termed dynamin GTPase effector domain (GED) (Schmid & Frolov, 2011). So far, the only intermolecular GAP that has been identified for dynamin is phospholipase D (PLD), which selectively regulates EGFR but not Tf endocytosis (Lee *et al*, 2006; Padrón *et al*, 2006). Interestingly, some other dynamin-interacting proteins also regulate selective endocytosis, including growth factor receptor-bound protein 2 (Grb2) that is essential for EGFR endocytosis and sorting nexin 9 (SNX9) that is required for Tf endocytosis (Martinu *et al*, 2002; Soulet *et al*, 2005). All of these raise the possibility that selective endocytosis is regulated at the late stage of endocytosis through cooperation between dynamin and its interacting proteins.

We and others previously characterized the actin-binding protein girdin (girders of actin filament) as a critical regulator of migration of endothelial cells, cancer cells, and neuroblasts, all of which depend on extracellular cues including growth factor stimulation (Enomoto *et al*, 2005, 2009; Le-Niculescu *et al*, 2005; Jiang *et al*, 2008; Kitamura *et al*, 2008; Ohara *et al*, 2012). Although girdin was reported to be a component of a protein complex that included dynamin (Simpson *et al*, 2005), the role of girdin in CME has not been investigated. Also, our previous finding that girdin colocalizes with submembranous actin network (Enomoto *et al*, 2005), which possess critical roles in CME (Kaksonen *et al*, 2006), led to the idea of girdin's involvement in CME.

In this study, we revealed that girdin regulates cargo-selective CME. Our results showed that girdin functions as an intermolecular GAP for dynamin 2 and is involved in the internalization of Tf and E-cadherin, but not EGFR or integrin β1. We also provide sets of data showing that the selective function of girdin in CME is achieved through (i) spatially controlled clathrin-coated pit (CCP) formation and (ii) competitive interaction among cargoes, dynamin, and girdin.

Results

Girdin interacts with dynamin 2

Previous study indicated girdin as the component of dynamin complex (Simpson *et al*, 2005). To confirm this finding, the endogenous interaction between girdin and dynamin was investigated by co-immunoprecipitation (Co-IP). We observed that the endogenous girdin/dynamin interaction could be detected in the presence of either GTPγS (a non-hydrolyzable GTP analogue) or GDP; however, dynamin preferentially interacted with girdin in the presence of GTPγS (Fig 1A), indicating that their interaction was regulated by GTP binding to dynamin. To further show that girdin is associated with dynamin, protein fractionation experiment was performed by gel filtration (Fig 1B). Consistent with our previous report, native girdin from HeLa cells was eluted with an apparent molecular mass much greater than that of the monomeric protein, which is mediated by self-oligomerization via girdin N-terminal (NT) and coiled-coil domains (Enomoto *et al*, 2005). Significantly, the elution pattern of girdin largely overlapped with that of dynamin, further supporting the idea that girdin interacts with dynamin *in vivo* (Fig 1B). Mapping the interacting domains indicated that the middle region (N2) of the girdin NT domain was responsible for the association with dynamin 2 (Fig 1C–E). Moreover, the GTPase and GED domains of dynamin 2 contained girdin-binding sites (Fig 1F). The interaction was further confirmed by *in vitro* binding assays using purified recombinant proteins, which revealed that girdin NT domain interacted with both dynamin GTPase and GED domain directly in a GTP-dependent manner (Fig 1G and H).

Girdin selectively regulates CME

Knowing that dynamin is a key regulator for endocytosis in eukaryotic cells, we asked whether girdin is also involved in this process using HeLa cervical carcinoma cells. The internalization of Tf, EGFR, integrin β1, and E-cadherin, which are internalized through CME (Paterson *et al*, 2003; Nishimura & Kaibuchi, 2007; Sigismund *et al*, 2008; Ezratty *et al*, 2009; Sato *et al*, 2011), was evaluated using confocal microscopy (Fig 2A and B) and antibody-capture enzyme-linked immunospecific assays (ELISA) after labeling cell surface proteins with sulfo-NHS-SS-Biotin (Fig 2C–F). The results revealed that RNA interference-mediated depletion (knockdown) of girdin reduced the internalization of Tf, although modestly, and E-cadherin, but not EGFR or integrin β1. The effect of girdin knockdown on Tf uptake was greater in the fluorescence-based assay than the ELISA assay (Fig 2B and C), which could be due to the different sensitivity between these assays. These data raised several questions: (i) how did girdin regulate CME and (ii) how did girdin selectively regulate the endocytosis of specific cargoes?

Girdin functions as a GAP for dynamin 2 to regulate CME

To address the mechanism for girdin-mediated regulation of CME, we first hypothesized that girdin regulates CME through interaction with dynamin. It is known that overexpression of protein interaction domains taken from endocytic proteins results in the dysregulation of CME (McMahon & Boucrot, 2011). We utilized this experimental system to test whether girdin regulated CME through interaction with dynamin 2. Tf internalization was inhibited by the overexpression of the girdin NT and N2 domains that are able to bind to dynamin 2, but not other domains (N1, N3, M1, M2, and CT) (Fig 3A–C). The effect of overexpressing the girdin NT domain was partly rescued by the expression of exogenous dynamin 2 (Fig 3B and C), further supporting the view that balanced and regulated interaction between dynamin 2 and girdin is essential for Tf endocytosis. In girdin-depleted cells, the expression of RNA-resistant wild-type girdin, but not its mutants lacking the NT domain (ΔNT), could restore Tf uptake (Supplementary Fig S1A and B), further proving that girdin regulates CME through interaction with dynamin 2.

We next examined whether girdin regulated dynamin 2 GTPase activity using a colorimetric GTPase assay (Quan & Robinson, 2005; Takahashi *et al*, 2010). This test indicated that the girdin NT domain increased the GTPase activity of dynamin 2 in a time- and dose-dependent manner (Fig 3D). Some SH3 domain-containing proteins, such as Grb2, increase dynamin GTPase activity indirectly

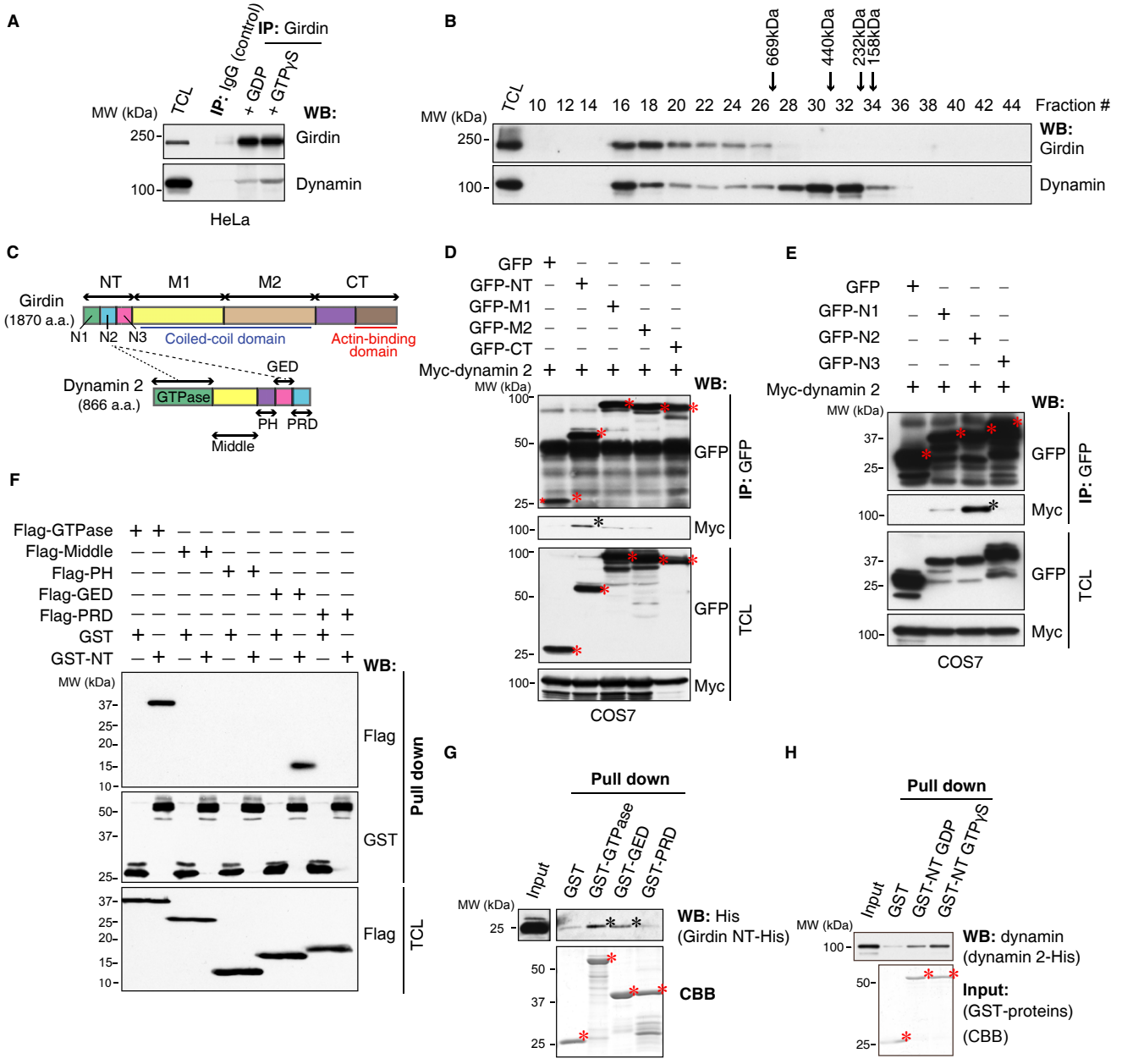

Figure 1. Interaction between girdin and dynamin.

A Co-IP illustrating the guanine nucleotide-regulated interaction between endogenous girdin and dynamin in HeLa cells. IP, immunoprecipitation; WB, Western blot.

B Whole-cell lysates from HeLa cells were loaded onto Superose 6 10/300 GL column for gel filtration. Following fractionation, each fraction was examined by Western blot analyses with anti-girdin (upper panel) and anti-dynamin (lower panel) antibodies to determine their elution profiles. The elution positions of calibration proteins with known molecular masses (kDa) are indicated, and an equal volume from each fraction was analyzed.

C Domain structures of human girdin and dynamin 2.

D, E The dynamin 2-binding site mapped to the N2 domain of girdin. Lysates from COS7 cells transfected with the indicated plasmids were immunoprecipitated with anti-GFP antibody. The girdin fragments and bound myc-dynamin 2 are indicated by red asterisks and a black asterisk, respectively. TCL, total cell lysate.

F The girdin-binding sites mapped to the GTPase and GED domains of dynamin 2. COS7 cells were transfected with the indicated combination of each domain of dynamin 2, GST, and GST-NT. The lysates were incubated with glutathione beads, followed by Western blot analysis. Dynamin 2 GTPase and GED domains that bound to GFP-NT are indicated by red asterisks.

G Direct interaction between the girdin NT domain and dynamin 2. The purified recombinant girdin NT (NT-His) was incubated with recombinant GST fusion proteins containing the GTPase, GED, and PRD domains of dynamin 2 conjugated to glutathione beads. The complexes were eluted with 1× SDS sample buffer, separated on SDS–PAGE, and subjected to Coomassie brilliant blue staining (CBB) and Western blot analyses using anti-His antibody. Red and black asterisks indicate GST fusion proteins and bound girdin NT, respectively.

H The *in vitro* binding assays indicated a direct interaction of the girdin NT domain with dynamin 2 in a guanine nucleotide-regulated manner. Purified recombinant dynamin 2 was diluted with GTPase IP buffer and loaded with GTPγS or GDP and then incubated with recombinant GST-NT conjugated to glutathione beads. The complexes were eluted, separated on SDS–PAGE, and subjected to CBB staining and Western blot analyses. Asterisks indicate GST fusion proteins.

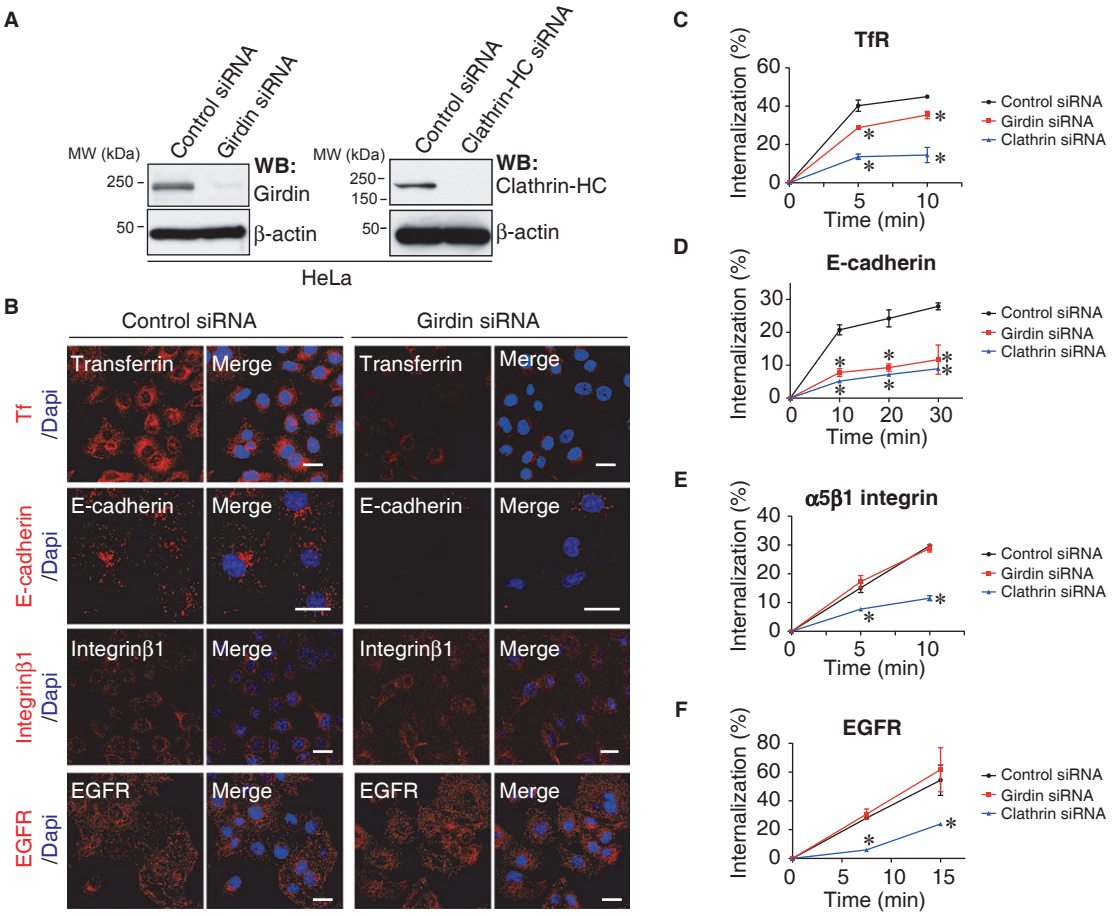

Figure 2. Girdin regulates selective endocytosis.

A Western blot evaluation of the knockdown efficiency of girdin and clathrin HC siRNAs in HeLa cells.

B The effect of girdin knockdown on the endocytosis of several cargoes (red) in HeLa cells was visualized using confocal microscopy. The nuclei were visualized by staining with 4′,6-diamidino-2-phenylindole (DAPI, blue). Scale bar, 20 μm.

C–F The effects of girdin knockdown on endocytosis were assessed using ELISA assays in which the knockdown of clathrin HC served as a positive control (blue). The asterisks indicate statistical significance compared with the control (black) ($P < 0.05$). Data are presented as means ± SE ($n = 3$).

via promoting the self-assembly of dynamin 2 into higher-ordered oligomers (Barylko *et al*, 1998). We found that, in contrast with Grb2, that binds to dynamin independently of GTPγS loading, girdin failed to increase the self-assembly of dynamin 2 into higher-ordered oligomers (Fig 3E and F). These results suggested that girdin functioned as an intermolecular GAP for dynamin 2 to directly increase its GTPase activity through a different mode of action compared to Grb2.

Comparative analysis of the sequences of the girdin NT domain and other GAP proteins led to the identification of several arginine residues that we predicted were essential for GAP activity (Supplementary Fig S1C). We purified mutant girdin proteins in which the arginines were replaced with alanines (R63A, R75A, R84A, R144A) in the NT domain. We then examined the function of those mutants by dynamin GTPase assays (Supplementary Fig S1C). We found that two mutations (R63A and R84A) significantly reduced the GTPase activity of dynamin versus the wild type. In accord with this, re-expression of the girdin double alanine mutant (R63A/R84A) could not restore Tf uptake in girdin-depleted cells (Supplementary Fig S1A and B). These results further supported the critical role of those two arginines in girdin's function as a GAP for dynamin.

The importance of girdin in CME was further demonstrated by transmission electron microscopic analysis. These studies revealed that the morphology of electron-dense CCPs and vesicles was deregulated in girdin knockdown cells (Fig 3G and H). This phenotype partially recapitulated abnormal tubulation and fission of CCPs found in cells expressing the dominant-negative mutant (K44A) of dynamin or dynamin-deficient cells (Damke *et al*, 2001; Tosoni *et al*, 2005; Ferguson *et al*, 2009), further implicating the importance of girdin/dynamin 2 interaction in the proper fission of CCPs.

Selective scission of CCPs by a competitive mechanism that involves girdin

Dynamin 2 is ubiquitously expressed and non-selectively controls vesicle scission of all CCPs (Schmid & Frolov, 2011; Ferguson & De Camilli, 2012). Thus, the above data indicating that girdin functioned as a GAP for dynamin 2 cannot explain how girdin selectively

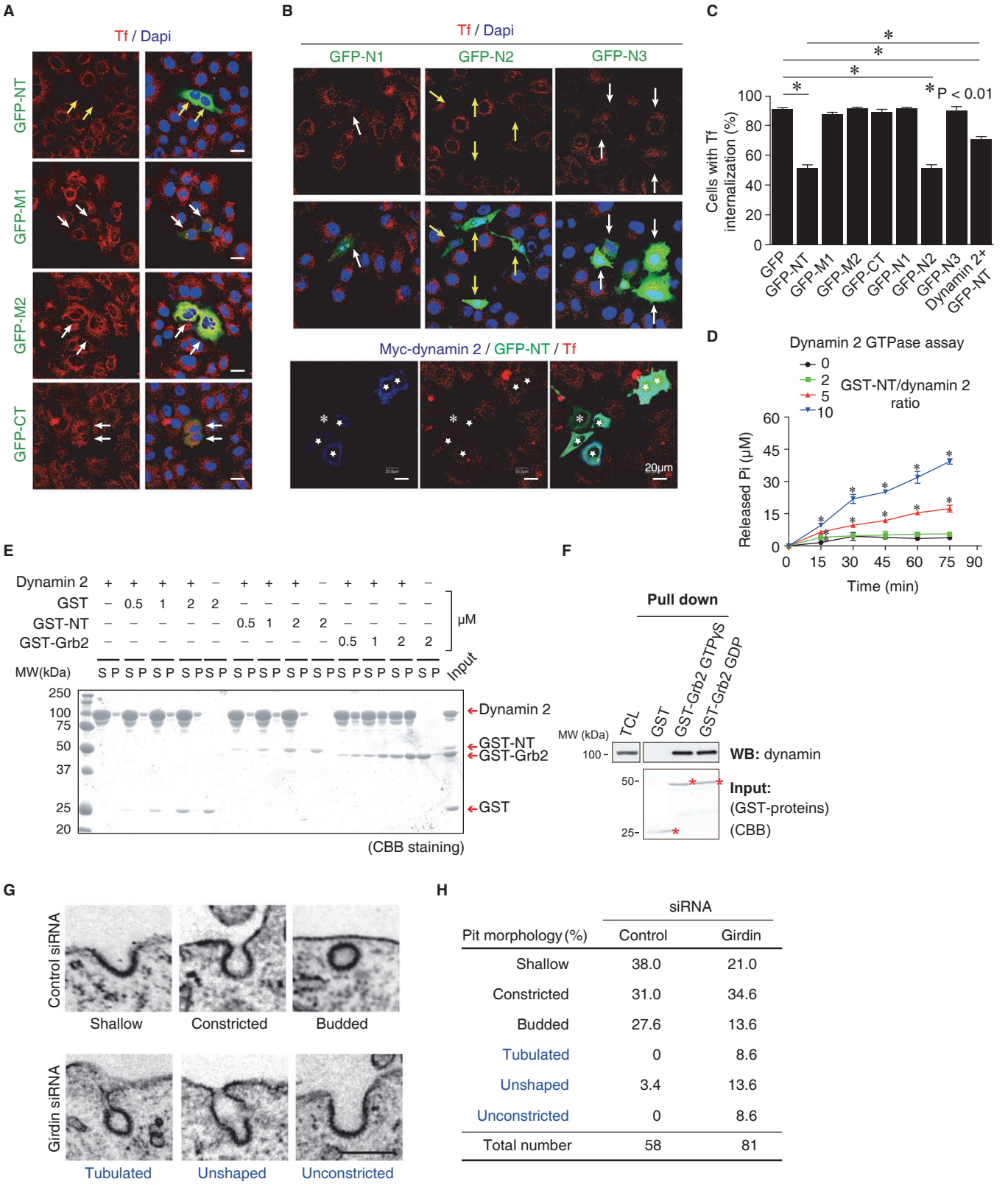

Pit morphology (%)	siRNA Control	siRNA Girdin
Shallow	38.0	21.0
Constricted	31.0	34.6
Budded	27.6	13.6
Tubulated	0	8.6
Unshaped	3.4	13.6
Unconstricted	0	8.6
Total number	58	81

regulated endocytosis and suggested the existence of other mechanisms. Previous studies have revealed that a CCP subpopulation located at the cell periphery is responsible for EGFR endocytosis, suggesting that different CCPs contain distinct cargoes and selective endocytosis may be spatially controlled (Miaczynska *et al*, 2004; Tosoni *et al*, 2005; Lakadamyali *et al*, 2006; Leonard *et al*, 2008;

Figure 3. Girdin regulates endocytosis as a dynamin 2 GAP.

A–C The GFP-fused domains or fragments of girdin were transfected into HeLa cells, followed by Tf internalization assays. Note that the cells transfected with GFP-NT or GFP-N2 (yellow arrows) but none of the other domains or fragments (white arrows) demonstrated decreased Tf internalization compared with non-transfected cells. In the experiment shown in the lower panel of (B), dynamin 2 expression partially rescued the defects in Tf internalization in cells overexpressing GFP-NT. Note that cells expressing both GFP-NT (green) and myc-dynamin (blue) tended to restore Tf internalization (indicated by the stars) compared with cells transduced only with GFP-NT (indicated by an asterisk). The percentage of cells with internalized Tf in each group (100 cells from three independent experiments) is quantified in (C). Scale bar, 20 μm. Data are presented as means ± SE (n = 3).

D Dynamin GTPase activity assays demonstrated that the girdin NT domain increased dynamin 2 GTPase activity in a time- and dose-dependent manner. The numbers indicate the molar ratio of GST-NT to dynamin 2 used in this assay. The asterisks indicate statistical significance compared with control ($P < 0.05$). Data are presented as means ± SE (n = 3).

E The self-assembly of dynamin 2 was assessed using velocity sedimentation, followed by SDS–PAGE analysis of the pellets (P) and supernatants (S). Assembled dynamin 2 was discovered in the pellet fraction. GST and GST-Grb2 were used as negative and positive controls, respectively.

F The interaction between dynamin and Grb2 was not regulated by nucleotide binding to dynamin. HeLa cell lysates were loaded with GTPγS or GDP and then incubated with recombinant GST-Grb2 conjugated to glutathione beads. Asterisks indicate GST fusion proteins.

G Representative transmission electron microscopic images of shallow, constricted, and budded CCPs (control HeLa cells) and tubulated, unshaped, and unconstricted CCPs (girdin knockdown cells). Scale bar, 250 nm.

H Morphometric analysis of electron microscopic images of CCPs shows the accumulation of tubulated, unshaped, and unconstructed pits in girdin knockdown cells.

Zoncu *et al*, 2009). We confirmed this notion by visualizing the endocytic sites of different cargoes using total internal reflectance fluorescence (TIRF) microscopy, which illuminates the bottom 100–200 nm of the cell (Fig 4A). Our data indicated that Tf and E-cadherin were internalized diffusely throughout the cells, whereas integrin β1 and EGFR endocytosis were mediated by peripheral CCPs, hinting at the idea that girdin may be involved in the endocytosis of CCP subpopulation that include distinct type of cargoes. In our observation by TIRF microscopy, however, girdin colocalized, at least partially, with endocytic sites for all of the four cargoes tested (Supplementary Fig S2A–D), suggesting that colocalization per se is not sufficient to determine the selectivity for the cargoes.

A clue in revealing the mechanism for girdin-mediated selective CME has come from a previous study, which showed that girdin bound to EGFR through its NT domain, leading to the modification of the EGFR signaling (Ghosh *et al*, 2010). We hypothesized that, in EGFR-containing CCPs, the competition between EGFR and dynamin 2 for interaction with girdin inhibited dynamin 2/girdin interaction, which makes the EGFR endocytosis out of regulation by girdin. Indeed, co-IP experiments using antibodies recognizing the extracellular domain of cargoes indicated that girdin interacted with EGFR and integrin β1, the endocytosis of which was not regulated by girdin (Fig 4B). In contrast, girdin did not efficiently bind with TfR or E-cadherin, the endocytosis of which is prone to regulation by girdin (Fig 4B and C). Interestingly, the knockdown of clathrin or dynamin 2 did not affect the interaction between girdin and EGFR or integrin β1 (Supplementary Fig S2E), indicating that these interactions occurred prior to and independently of dynamin-mediated scission of membranes. Binding assays using purified proteins exhibited direct interaction of the girdin NT domain with the cytoplasmic domains of both EGFR and integrin β1 (Fig 4D and E), which competitively inhibited dynamin 2/girdin interaction in a dose-dependent manner (Fig 4F and G). Taken together, these data suggest that the competitive mechanism, which prevented girdin from interacting with dynamin 2 and executing its GAP function in EGFR- or integrin β1-positive CCPs, contributed to the selective nature of endocytosis (Fig 7).

Girdin spatially controls CCP formation

We next examined the localization of girdin in HeLa cells at the ultrastructural level by quick-freeze deep-etch electron microscopy, which detected girdin surrounding CCPs throughout the early to late stages of CME (Fig 5A, and Supplementary Fig S3A–C). TIRF observation confirmed that endogenous girdin partially colocalized with clathrin adaptor AP-2 that is one of the CCP markers (Supplementary Fig S3D). Also, consistent with our biochemical data that the girdin NT domain is responsible for the binding with dynamin 2, we observed the consistent colocalization of the girdin NT domain, but not other girdin domains, with AP-2 and clathrin heavy chain (HC), on the cell membrane (Fig 5B, and Supplementary Fig S3E and F). Interestingly, TIRF observation revealed that girdin knockdown significantly reduced the density of AP-2/clathrin HC-positive CCPs in the center of cells but had no effect on the formation of CCPs at the cell periphery (Fig 5C), implicating the involvement of girdin in spatial control of CCP formation. The heterogeneous distribution of CCPs induced by girdin knockdown was more apparent in cells defective for Tf internalization, as they exhibited accumulation of CCPs at the cell periphery and few CCPs formed in the centers of such cells (Fig 5D and E). These data suggest that girdin's function seems to be involved in spatial control of CCP formation.

Time-lapse TIRF recordings revealed that girdin was consistently located at CCPs even before the nucleation stage of CME (Fig 5F, Supplementary Fig S4A and Supplementary Video S1), suggesting the possible involvement of girdin in the early steps of CCP formation. It is of note that previous studies have shown that the knockdown of clathrin or dynamin inhibits CME without affecting the recruitment of AP-2 to the CCPs, which indicates that different CCP components are recruited there and regulated at distinct stages (McMahon & Boucrot, 2011). Consistent with this notion, we observed that colocalization between girdin and AP-2 was not affected by the knockdown of clathrin or dynamin 2 (Supplementary Fig S4B), which further confirmed girdin's role in the early stage of CME. Next, to know how girdin controls CCP formation, we tested the possibility that girdin had the capacity to bind to and recruit the constituents of CCPs such as the AP-2 protein complex. Co-IP experiments showed that girdin interacted with the AP-2 α subunit, although whether the interaction was direct or indirect was not determined (Fig 5G). The data indicated that via an unknown mechanism, girdin participated in central CCP formation partially through recruitment of the AP-2 protein complex.

Because different cargoes were internalized via different subpopulation of CCPs (Fig 4A), we speculated that girdin also

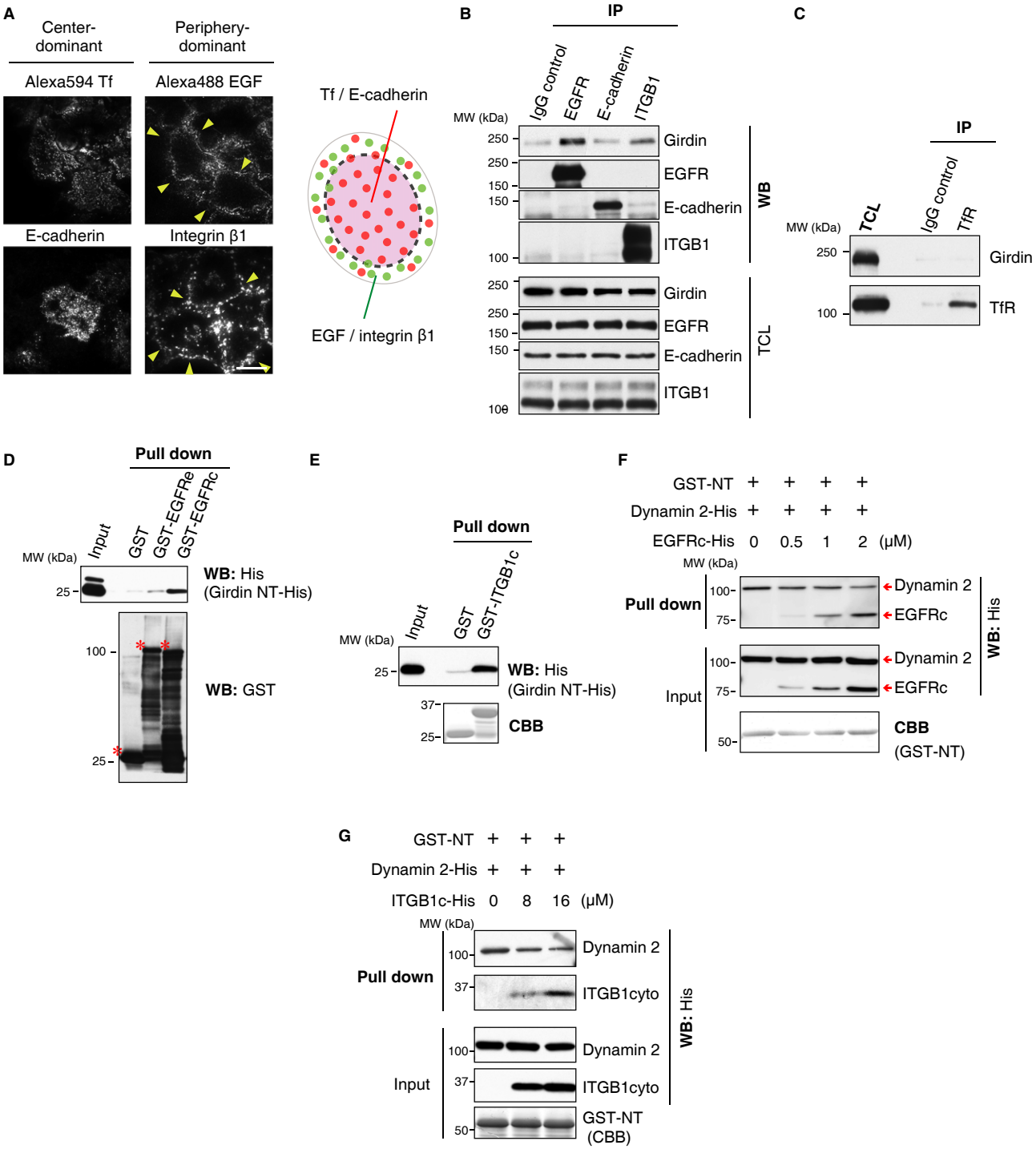

Figure 4. Possible involvement of competition between cargoes and dynamin for binding to girdin in selective control of CME.

A The endocytic sites for the indicated cargoes were investigated using TIRF microscopy according to the methods described in the Materials and Methods section. Arrowheads indicate vesicles responsible for EGF and integrin β1 internalization at the periphery of the cells. Scale bar, 20 μm. Shown in the right panel is the illustration indicating the endocytic sites for each cargo. See also Supplementary Fig S5A.

B, C HeLa cell lysates were subjected to immunoprecipitation by the indicated antibodies, followed by Western blot analysis. The results showed that girdin interacts with EGFR and integrin β1 but not E-cadherin or TfR.

D, E *In vitro* binding assays using purified recombinant proteins demonstrated the direct interaction of girdin NT with the cytoplasmic domains of EGFR (EGFRc) (D) and integrin β1 (ITGB1c) (E) but not the extracellular domain of EGFR (EGFRe). In (D), the precipitated GST fusion proteins are indicated by asterisks.

F, G The dose-dependent competition of EGFR and integrin β1 for the binding of dynamin 2 to the girdin NT domain. GST-fused girdin NT (3 μg) was incubated with dynamin 2-His (30 μg) in the presence of increasing amounts of EGFRc-His (F) or ITGB1c-His (G). The mixtures of the proteins were precipitated with glutathione Sepharose beads, followed by Western blot analysis.

specifically regulates endocytosis occurred in cell center through controlling CCP formation in this region. Indeed, compared with control cells (Fig 4A), we found that girdin knockdown affected Tf internalization in the center of cells, maintaining Tf and EGF endocytosis at the cell periphery (Fig 5H, and Supplementary Fig S5A and B). Consistent with this finding were observations made by immunoelectron microscopic analysis that revealed that girdin knockdown led to a defect of the localization of Tf receptor (TfR), but not EGFR, on clathrin-coated vesicles (CCVs), suggesting the involvement of girdin in selective endocytosis (Supplementary Fig S5C and D). In addition, consistent with a previous report that dynamin-null cells had normal CCP formation (Ferguson *et al*, 2009), we also found the overexpression of the dynamin K44A mutant did not affect the formation of CCPs (Supplementary Fig S5E), which was not identical to changes induced by girdin depletion (Fig 5C). Thus, these results indicate that, besides competitive mechanism involving dynamin, girdin also regulates spatially controlled endocytosis in distinct regions of cells, which must be distinguished from its function as a GAP for dynamin 2.

Girdin-mediated selective endocytosis is involved in maintaining cell polarity

Finally, to investigate the physiological function of girdin-mediated selective endocytosis, we studied the involvement of girdin in the establishment of epithelial cell polarity, which is determined by endocytosis (Wirtz-Peitz & Zallen, 2009; Levayer *et al*, 2011). To this end, we utilized Madin–Darby canine kidney (MDCK) cells, which have polarized endocytic trafficking with apical-basolateral protein sorting. Knockdown of girdin in MDCK cells depolarized the localization of TfR and E-cadherin, but had no effect on the localization of integrin β1 (Fig 6A, B and E). Of note, the localization of E-cadherin at the basal membrane was significantly deregulated with patchy distribution, especially in the cells defective for Tf endocytosis (Fig 6C–E). These data highlight the relationship between girdin-mediated selective endocytosis and polarized cellular function.

Discussion

In this study, we revealed that a new dynamin GAP protein girdin regulated cargo-selective CME via a novel mechanism (Fig 7). Girdin preferentially regulated CME that occurred in central cell membranes by controlling CCP formation, although its mechanisms remain unknown at present. In addition, girdin also selectively controlled the scission of CCPs in this area via competition between cargoes, dynamin, and itself. However, the generality of our hypothesis in other cargo-selective endocytosis remains to be proven, which should await further studies.

Dynamin is an atypical multidomain GTPase containing a large GTPase domain, which is well known for its critical role in budding or scission of transport vesicles (Schmid & Frolov, 2011; Ferguson & De Camilli, 2012). Distinct from other GTPases, previous biochemical studies and recent structural analyses showed that its GTPase catalytic activity is stimulated by oligomerization, which requires the involvement of the middle domain and the GED domain, where the GED domain serves as an intramolecular GAP to regulate its GTPase activity (Chappie *et al*, 2011; Faelber *et al*, 2011). However, how dynamin GTPase activity is regulated in cells is unclear. Although many Src homology 3 domain-containing proteins, such as Grb2 and SNX9, stimulate dynamin GTPase activity, they are not GAPs because they increase GTPase activity indirectly via modulating the oligomerization of dynamin by interacting with its proline-rich domain (PRD) (Gout *et al*, 1993). So far, the only intermolecular GAP that has been identified is PLD, which increases dynamin GTPase activity directly to regulate EGFR endocytosis (Lee *et al*, 2006). In the current study, we identified girdin as a second intermolecular GAP for dynamin. Interestingly, it seems that the functions of these two dynamin GAPs are complementary to each other. In contrast to PLD, girdin was required for Tf endocytosis but not EGFR, indicating the possibility that selective CME is differentially regulated by dynamin and its different types of GAPs.

Although many types of cargoes are internalized via CME, they are not competitive even in the same area of a cell, indicating that the endocytosis of different cargoes is differentially controlled. It has been suggested that selective CME is achieved through cargo-specific adaptors that interact with and recruit specific cargoes to CCPs (Traub, 2009). One concern about this hypothesis is that, considering the huge number of cargoes, it is impossible for cells to evolve an equivalent number of adaptors. Previous studies found that the CCPs on the cell membrane are functionally heterogeneous, that is, peripheral CCPs are utilized by EGFR for its internalization and transition to APPL1 (adaptor protein containing pleckstrin homology domain, PTB domain and leucine zipper motif 1)-positive endosomes. In contrast, central CCPs are responsible for Tf endocytosis (Miaczynska *et al*, 2004; Tosoni *et al*, 2005; Lakadamyali *et al*, 2006; Leonard *et al*, 2008; Zoncu *et al*, 2009). However, how this heterogeneity is determined and whether this contributes to selective endocytosis are unknown. In our study, we showed that girdin might be involved in the determination of the functional heterogeneity of CCPs. Girdin consistently localized around the sites of CCPs on the membrane to control the formation of CCPs in the center of cells. Accordingly, the knockdown of girdin induced the accumulation of CCPs around the cell periphery.

At present, the mechanism by which girdin spatially controls CCP formation in the center of cells but not the periphery is unknown and should be addressed in further. Recently, two studies have systematically identified the CCV components using proteomic approaches (Borner *et al*, 2006, 2012). Although girdin has not been identified in the hit list in those studies, it is tempting to see the difference between CCVs in control and girdin knockdown cells using the same approach, which will be helpful to uncover how girdin spatially regulates the formation of heterogeneous CCPs.

We propose that heterogeneity of CCPs is another mechanism for selective CME. CCP heterogeneity makes it possible for Tf and E-cadherin to be internalized in the central regions of cells through the action of girdin, whereas EGFR and integrin β1 can be internalized via CCPs at the cell periphery independent of girdin (Fig 7). Together, selective CME is achieved by heterogeneous CCPs and the corresponding dynamin GAP girdin, which seems to be crucial for cellular functions such as establishment of cell polarity that depends on the endocytic pathway (Fig 6). Interestingly, several genomewide screen studies identified that cell polarity proteins such as Par-6 (partitioning defective 6 homolog) and Cdc42 were involved in the

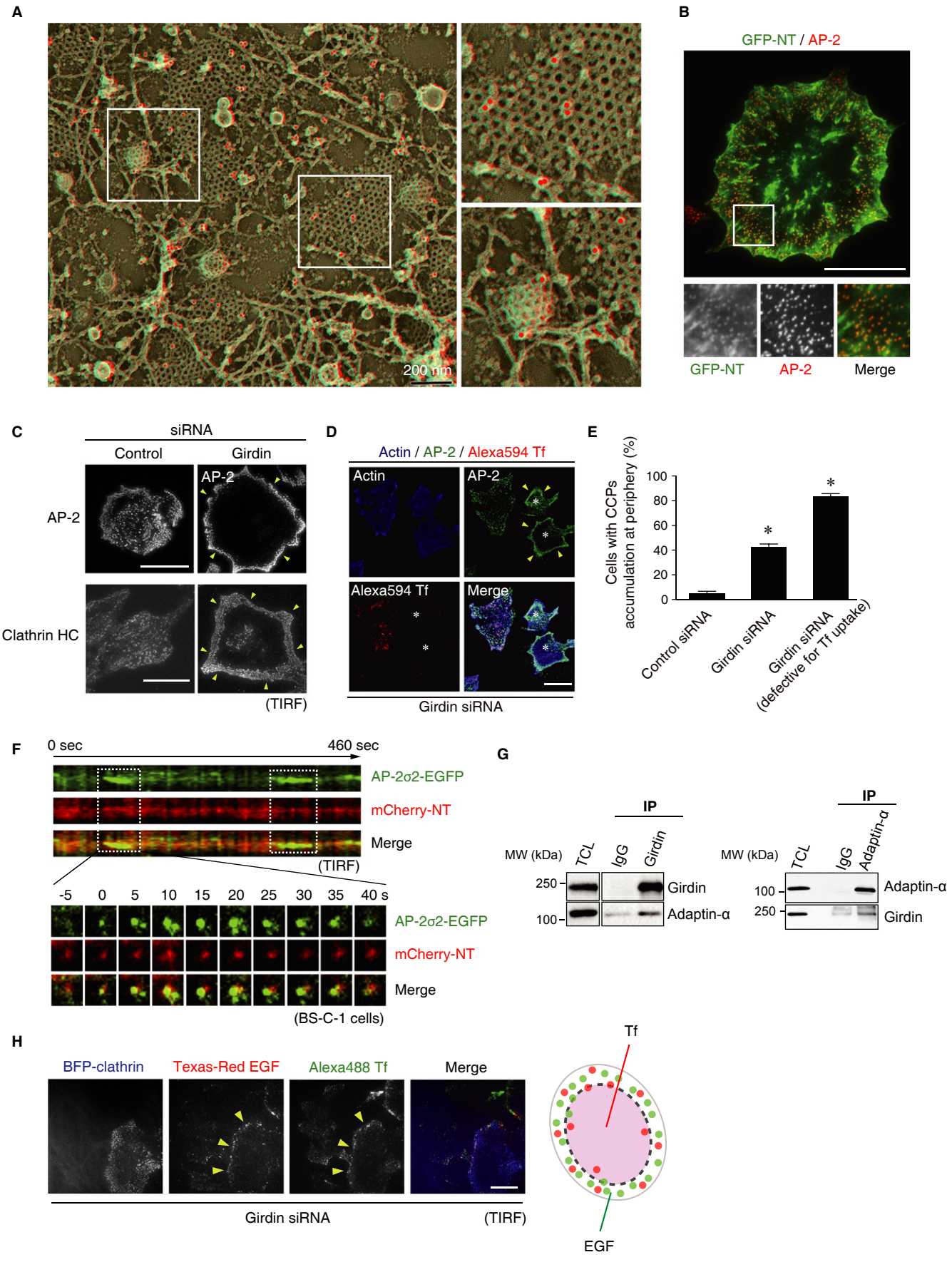

Figure 5. Girdin regulates CCP formation in the central regions of the cells.

A Ultrastructural analysis performed using quick-freeze deep-etch electron microscopy of unroofed cells. Immunogold labeling, which exhibited a clear dot surrounded by a halo of platinum–carbon coating (pseudo-colored red), revealed that girdin molecules localized with CCPs. The regions within the boxes are shown at a higher magnification in adjacent panels. Scale bar, 200 nm.

B GFP-NT (green)-expressing HeLa cells were fixed and stained for AP-2 (red). The region within the box is shown at a higher magnification in lower panels. Scale bar, 20 μm.

C HeLa cells transfected with control or girdin siRNA were stained with the indicated antibodies, followed by TIRF microscopic analysis. Girdin knockdown affected the formation of AP-2/clathrin HC-positive CCPs in the center of the cells, maintaining those in the cell periphery intact. Arrowheads indicate the CCPs accumulated at the cell periphery. Scale bar, 20 μm.

D, E Tf internalization (red) and AP-2 localization (green) were examined in girdin knockdown HeLa cells. Note that girdin knockdown cells defective for Tf internalization exhibited fewer CCPs in the centers of the cells, leading to accumulation of CCPs at the cell periphery (indicated by asterisks). In (E), the percentages of cells with CCP accumulation at the cell periphery were evaluated in control cells, girdin knockdown cells, and girdin knockdown cells with defective Tf internalization (100 cells from three independent experiments). The asterisks indicate statistical significance compared with the control cells ($P < 0.05$). Data are presented as means ± SE ($n = 3$). Scale bar, 20 μm.

F Kymograph (top) of a representative endocytic CCPs labeled with mCherry-NT (red) in BS-C-1 cells stably expressing AP2 σ2-GFP (green). This site showed two lifetimes of the CCP within the observed interval of 460 s, as indicated by the dotted boxes. Shown below are sequential images of the dynamic localization of mCherry-NT and AP2 σ2-GFP in the first lifetime of the CCP.

G Co-IP experiments illustrating the interaction of girdin with the AP-2 α subunit (adaptin-α) in HeLa cells.

H HeLa cells transfected with BFP (blue fluorescent protein) clathrin and girdin siRNA were incubated with fluorescence-conjugated EGF and Tf to induce their internalization, followed by observation of endocytic sites using TIRF microscopy. Arrowheads indicate CCPs responsible for EGF and Tf internalization at the periphery of the cells. Shown in the right panel is the illustration indicating the endocytic sites for each cargo. Scale bar, 20 μm.

endocytic pathway (Balklava *et al*, 2007; Collinet *et al*, 2010; Kozik *et al*, 2013). We previously reported that girdin interacted with the Par-3/Par-6/atypical protein kinase C protein complex to determine cell polarity during cell migration (Ohara *et al*, 2012), which further implicates the linkage between endocytosis and cell polarization and the involvement of girdin in both processes.

Knowing that girdin spatially controlled the formation of CCPs, we also examined whether girdin spatially regulated CCP scission as a GAP of dynamin. Based on our results, we found that girdin interaction with some cargoes, such as integrin β1 and EGFR, competitively disrupted dynamin 2/girdin interaction, which prevented girdin from executing its GAP function. Thus, it had no function in the scission of integrin β1/EGFR-containing CCPs at the cell periphery. We note that more recombinant integrin β1 is required for competitively disrupting the dynamin 2/girdin interaction compared with EGFR (Fig 4F and G), which may reflect the difference in the stoichiometry and affinity between girdin and these cargoes. It is well known that cargoes determine the fate of CCPs (Loerke *et al*, 2009; Liu *et al*, 2010; Mettlen *et al*, 2010; Henry *et al*, 2012). Here, we showed that cargoes also determine the specificity of CME at the scission stage, which challenges the earlier common view that the specificity of CME is determined only in the early stages of CME.

In summary, in this study, we revealed girdin, a dynamin GAP, regulates selective endocytosis in a new spatial regulatory mechanism. Further identification of other dynamin GAPs and their interacting cargoes is necessary to determine whether this mechanism is a general feature of other selective, accurate, and efficient CMEs targeting different types of cargoes.

Materials and Methods

Cell culture, transfection, and RNAi

HeLa, COS7, and MDCK cells were purchased from American Tissue Type Culture (Rockville, MD) and cultured in Dulbecco's modified Eagle's medium (DMEM) supplemented with 10% fetal bovine serum (FBS). BS-C-1 cells stably expressing AP-2 σ2-EGFP or LCa (clathrin light-chain A)-EGFP (Ehrlich *et al*, 2004) were kindly provided by Tomas Kirchhausen (Harvard Medical School) and cultured in DMEM supplemented with 10% FBS and 1 mg/ml of geneticin (Invitrogen). siRNA or plasmids were transfected into cells using Lipofectamine 2000 (Invitrogen) according to the manufacturer's instructions. Lipofectamine LTX (Invitrogen) or FuGene HD (Roche Diagnostics, Indianapolis, IN) was used to obtain a high expression level of plasmid in HeLa or BS-C-1 cells, respectively. The targeted sequences of siRNA used in this study, the specificity of which has been previously demonstrated, were as follows: girdin (5′-AAGAAGGCTTAGGCAGGAATT-3′), clathrin heavy chain (5′-AA TCCAATTCGAAGACCAATT-3′), dynamin 2 (5′-CTGCAGCTCATCTTC TCAAAA-3′). For short hairpin RNA (shRNA)-mediated knockdown of girdin, the targeted sequence 5′-GAAGGAGAGGCAACTGGAT-3′ was inserted into pSIREN-RetroQ retroviral shRNA expression vector (Clontech, Palo Alto, CA) as previously described (Enomoto *et al*, 2009; Ohara *et al*, 2012).

Plasmids

The construction of plasmids encoding GFP-girdin fragments, pEF-BOS-GST, and pEF-BOS-GST-Girdin-NT, were previously described (Enomoto *et al*, 2005, 2009). cDNA fragments encoding the girdin NT (1–256) or integrin β1 cytoplasmic domain (752–798) were inserted into the pGEX-5X-2 vector (GE Healthcare, Waukesha, WI) or pET-21a vector (Novagen, Madison, WI). The pGEX-4T-2-Grb2, pGEX-4T-2-EGFRe (extracellular domain), and pGEX-4T-2-EGFRc (cytoplasmic domain) plasmids were previously generated in our laboratory. cDNAs encoding human dynamin 2, which were purchased from Open Biosystems (Huntsville, AL), were inserted into the pEF1/Myc-His A (Invitrogen) or pET-21a vector. cDNA encoding the EGFR cytoplasmic domain (669–1210) was inserted into the pET-24d vector. cDNA encoding human dynamin 2 was inserted into the pRetroQ-AcGFP vector (Clontech). cDNA encoding human dynamin 2 GTPase (1–300), Middle (301–518), PH (519–625), GED (626–744), or PRD (745–867) domains were subcloned into the pFlag-CMV-2 vector (Sigma). cDNA encoding the clathrin light-chain A (generously provided by Katsuhiro Kato, Nagoya

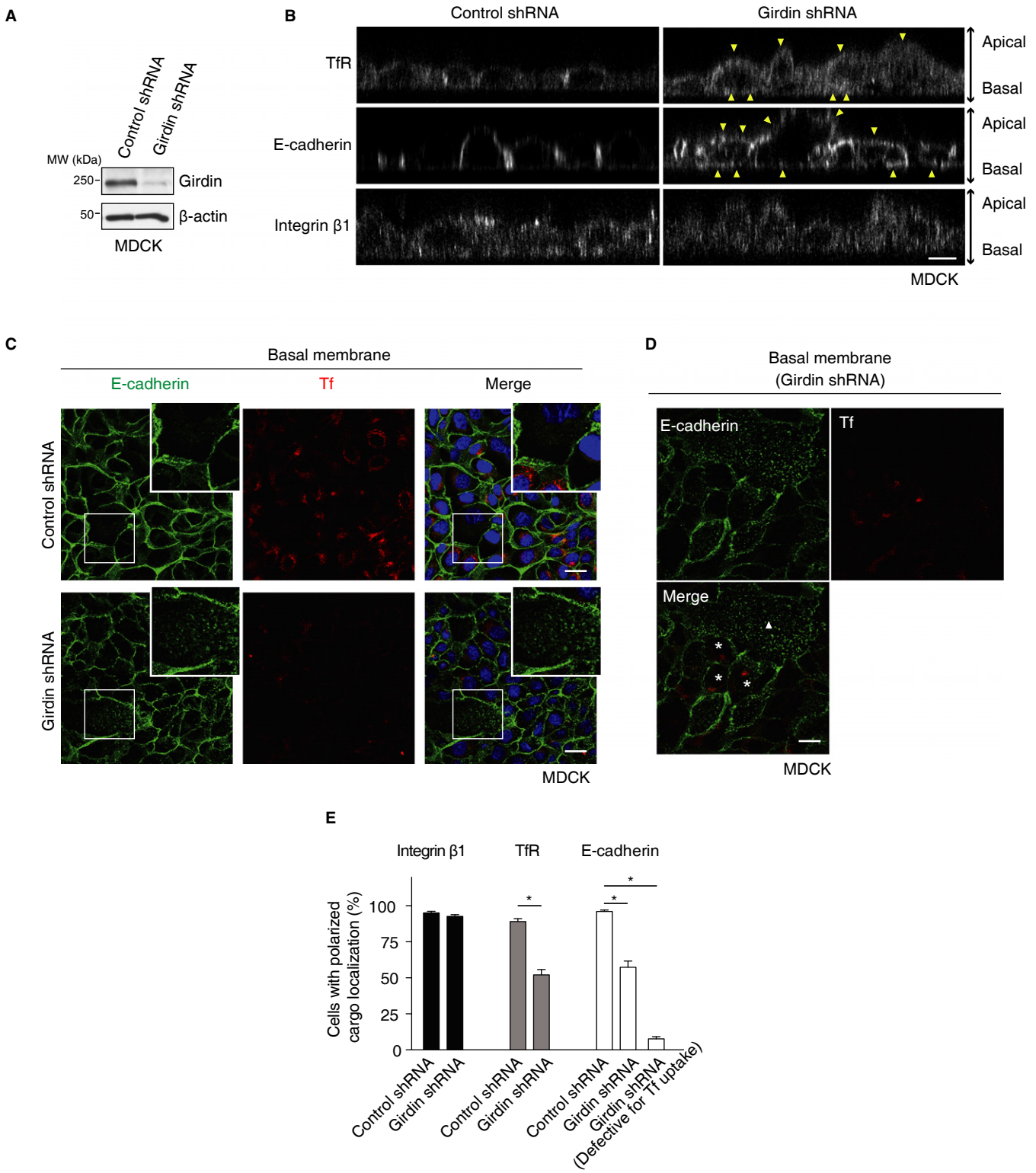

University) was inserted into the pTagBFP vector (Evrogen, Moscow, Russia). cDNA encoding E-cadherin was inserted into the pRetroQ-AcGFP-C1 vector to replace the sequence encoding AcGFP. To generate mCherry-girdin-NT plasmid, the GFP sequence in pcDNA3.1-GFP-girdin-NT was substituted with the mCherry sequence.

Endocytosis assays

Cargo endocytosis was investigated using conventional immunofluorescent imaging technique. For the evaluation of transferrin internalization, HeLa cells starved in binding buffer (DMEM containing 20 mM HEPES and 0.1% BSA) for 3 h were incubated with 50 μg/ml

Figure 6. Girdin-mediated selective endocytosis regulates polarized localization of TfR and E-cadherin in epithelial cells.

A Western blot evaluation of the knockdown efficiency by girdin shRNA in MDCK cells.

B Knockdown of girdin depolarized the localization of TfR and E-cadherin in MDCK cells (upper and middle panels). In control cells, TfR and E-cadherin were mainly located around the cell–cell contact sites. In contrast, in girdin knockdown cells, TfR and E-cadherin were not limited to the cell–cell contact sites, as they were also localized at the basal and apical membranes (arrowheads). Note that girdin knockdown had no apparent effect on the localization of integrin β1 (lower panel). Scale bar, 20 μm.

C, D MDCK cells starved and incubated with Alexa-594-conjugated Tf (red) were stained by E-cadherin antibody (green), followed by the visualization of the basal membrane by confocal microscopy. In control cells (C, upper panel), E-cadherin localized at the cell–cell contact sites. In contrast, in girdin knockdown cells that were defective for Tf endocytosis (C, lower panel), E-cadherin was preferentially located at the basal membrane in a dotted manner (lower panel, inset). The regions within the boxes are shown at a higher magnification in insets. Shown in (D) is another representative image of girdin-depleted cells taken from the same experiment. Note that in the cells with intact and defective Tf endocytosis (marked with asterisks and triangle, respectively), E-cadherin was localized at the cell–cell contact sites and the basal membrane, respectively. The data indicated the relationship between girdin knockdown efficiency and polarized localization of E-cadherin. Scale bar, 20 μm.

E The number of cells with polarized localization for each cargo in (B–D) was counted and quantified. The asterisks indicate statistical significance ($P < 0.05$). Data are presented as means ± SE ($n = 3$).

of Alexa-594-conjugated transferrin (Invitrogen) diluted in binding buffer at 37°C for 10 min, washed using ice-cold PBS, washed using acid buffer (0.5 M NaCl, 3% acetic acid) on ice to remove surface-bound transferrin, and then subjected to immunofluorescence studies using the confocal microscope. In assays investigating EGFR, integrin β1, and E-cadherin endocytosis, cells starved in the binding buffer for 3 h were incubated with either anti-EGFR (Santa Cruz Biotechnology, clone 528; 5 μg/ml), anti-integrin β1 (Santa Cruz Biotechnology, clone P5D2; 5 μg/ml), or anti-E-cadherin (TaKaRa, clone HECD-1; 2 μg/ml) antibody in ice-cold binding buffer on ice for 1 h. The cells were washed using ice-cold PBS three times and incubated with warmed binding buffer at 37°C for 10 min to stimulate cargo internalization. In the experiments testing EGFR endocytosis, a binding buffer containing 2 ng/ml EGF was used to ensure EGFR internalization through clathrin-mediated endocytosis. The cells were washed using ice-cold PBS and acid buffer to remove surface-bound antibodies; they were then fixed, permeabilized, and incubated with secondary antibodies and used for fluorescence imaging studies. The HeLa cells stably expressing E-cadherin were used in the experiments testing E-cadherin endocytosis.

In the experiments examining the endocytic sites of cargoes, the cells starved in the binding buffer for 3 h were incubated with 50 μg/ml fluorochrome-conjugated transferrin, 1 μg/ml fluorochrome-conjugated EGF, 5 μg/ml of anti-integrin β1 antibody, or 2 μg/ml anti-E-cadherin antibody in the binding buffer for 10 min. The cells were washed with ice-cold PBS, fixed, permeabilized, and incubated with secondary antibodies, and then, the bottom of the cells was observed using the TIRF system.

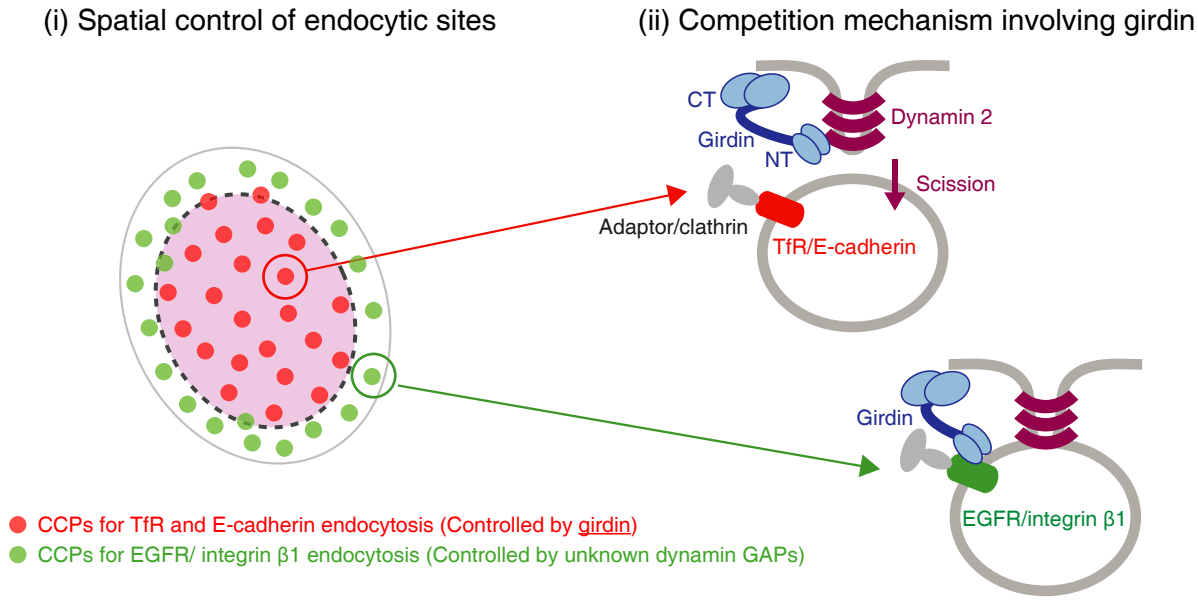

Figure 7. A proposed model for spatially controlled selective endocytosis regulated by girdin.

A proposed model for spatial control of CME by dynamin GAP girdin and its specific interaction with cargoes conferring the selectivity for CME. The dynamin 2 GAP protein girdin preferentially controlled CME that occurred in the center of cells by controlling the formation of CCPs, although the mechanism remains unclear at present. In TfR- or E-cadherin-containing CCPs, girdin functioned as a GAP for dynamin 2, resulting in the scission of CCPs. In contrast, girdin interacted with the cytoplasmic region of those cargoes in EGFR- or integrin β1-containing CCPs, inhibiting the dynamin 2/girdin interaction. In that case, other unknown dynamin GAPs would be mobilized to regulate dynamin activity.

Quantification of cargo endocytosis

Cells starved in the binding buffer for 3 h were quickly washed twice using ice-cold PBS on ice and then incubated with 250 μg/ml of sulfosuccinimidyl-2-(biotinamido)ethyl-1,3-dithiopropionate (sulfo-NHS-SS-Biotin, Thermo Scientific) at 4°C for 30 min. The cells were washed three times using ice-cold PBS and incubated with binding buffer (or binding buffer containing 2 ng/ml of EGF in the assay used to examine EGFR endocytosis) at 37°C to allow internalization to occur. After internalization, the medium was aspirated, and the cells were transferred onto ice and washed twice using ice-cold PBS. Surface-bound biotin was removed via incubation with stripping buffer (20 mM sodium 2-mercaptoethanesulfonate (MesNa), 50 mM Tris, 100 mM NaCl, pH 8.6) for 30 min. The cells were washed three times using ice-cold PBS, lysed in IP lysis buffer, and centrifuged. The biotinylated cargoes in the supernatants were determined by a capture ELISA. For the ELISA assays, 96-well plates (Thermo Scientific, #439454) were pre-coated overnight with 50 μl of antibodies (5 μg/ml of anti-α5 integrin or anti-EGFR1 antibody, 2 μg/ml of anti-transferrin receptor or anti-E-cadherin antibody) in 50 mM Na_2CO_3 (pH 9.6) and blocked using 5% BSA in PBS-T at room temperature for 1 h. The plates were extensively washed using PBS-T, incubated overnight with 100 μl of cell lysates at 4°C, washed five times using PBS-T, and incubated with 1 μg/ml of streptavidin-peroxidase (Sigma, S5512) in PBS-T containing 1% BSA for 1 h. After washing, biotinylated cargoes were detected by means of a chromogenic reaction with ortho-phenylenediamine (Sigma, P5412). The reaction was terminated by adding 100 μl of 8 M H_2SO_4. The ELISA titers were calculated using optical density readings at 490 nm obtained using an Infinite M200 plate reader (Tecan, Research Triangle Park, NC).

Dynamin GTPase activity assays

A malachite green-based colorimetric dynamin GTPase activity assay was performed as previously described (Quan & Robinson, 2005; Takahashi *et al*, 2010). Purified histidine-tagged human or mouse dynamin 2 (0.39 μg/well, 100 nM) and GST fusion proteins (1,000 nM) were mixed in 5× dynamin diluting buffer (30 mM Tris–HCl, 100 mM NaCl, 0.1% Tween-80, pH 7.4) (8 μl per well) at room temperature for 30 min. During the incubation period, 32 μl of complete GTPase assay buffer (4 μl of 10× GTPase assay buffer [100 mM Tris–HCl, 100 mM NaCl, 20 mM $MgCl_2$, 0.5% Tween-80, pH 7.4], 4 μl of 10× leupeptin [10 μg/ml in distilled water], 4 μl of 10× phenylmethyl sulfonyl fluoride (PMSF) [1 mM in distilled water], 4 μl of 10× GTP [3 mM GTP (Cytoskeleton, Denver, CO) in 20 mM Tris–HCl, pH 7.4] and 16 μl of distilled water) was added to 96-well plates. The plates were incubated on a Thermomixer Comfort (Eppendorf, Hamburg, Germany) with continuous shaking at a rate of 300 rpm at 30°C. Subsequently, 8 μl of protein mixture was added to each well, and the incubation was continued for the indicated times. The reaction was terminated by adding 10 μl of 0.5 M EDTA, and then 150 μl of malachite green reagent (1 mg/ml malachite green [Wako, Osaka, Japan] and 100 mg/ml ammonium molybdate tetrahydrate [Sigma] in 1 M HCl filtered through a 0.45 μm filter) was added to develop the color. The absorption spectra at 650 nm were measured using an Infinite M200 plate reader. To obtain a standard calibration curve, 8 μl of 5× phosphate standards (500, 250, 150, 100, 50, 25 and 5 μM NaH_2PO_4 in distilled water) was added to each well containing 32 μl of the complete GTPase assay buffer.

Dynamin sedimentation assays

Purified recombinant dynamin 2 (2 μM) was incubated in sedimentation buffer (10 mM HEPES, 2 mM $MgCl_2$, 150 mM KCl, pH 7.2) at room temperature for 30 min with increasing amounts of tested GST fusion proteins (GST, GST-NT, or GST-Grb2). The reaction mixture (50 μl) was centrifuged at 4°C for 10 min at 19,200 *g*. Equal volumes of the pellets and supernatant fractions were separated by SDS–polyacrylamide gels (SDS–PAGE), followed by Coomassie blue staining.

Freeze-replica electron microscopy of the cytoplasmic cell surface

Electron microscopy of the cytoplasmic surface of the cell membrane and immunolabeling of girdin molecules were performed as previously described (Enomoto *et al*, 2005). HeLa cells were cultured on glass coverslips (3 mm in diameter, standard #1 Matsunami, Osaka, Japan). Immediately after being unroofed from the apical cell membrane, the cells were fixed for 30 min in 2.5% glutaraldehyde in buffer A (70 mM KCl, 5 mM $MgCl_2$, 3 mM EGTA, 30 mM HEPES buffer adjusted at pH 7.4 with KOH). After being washed with buffer A/distilled water, specimens were quickly frozen with liquid helium by using the rapid-freezing device (Eiko, Tokyo, Japan, and Variant Instruments, MO, USA). Samples were then freeze-etched and rotary shadowed with platinum–carbon, in a newly developed freeze-etching device (FR9000, HITACHI, Ibaraki, Japan, and JEOL EM-1950 JFDII, Tokyo, Japan). For immunolabeling of girdin molecules, the unroofed cells were fixed for 30 min in 4% paraformaldehyde/0.5% glutaraldehyde in buffer A. After being washed three times with buffer B (100 mM NaCl, 30 mM HEPES, 2 mM $CaCl_2$), the samples were quenched and blocked, and then labeled for 1 h at 37°C with primary and secondary 10 nm gold-conjugated antibodies (Amersham, and BBI Solutions) in buffer B containing 1% BSA. Finally, specimens were rapidly frozen and freeze-etched as described above. The replica was separated, washed three times on water, and picked up on the forvar-coated EM grids. The replica was observed in JEOL JEM1200EX and 1400 (Tokyo, Japan) at 80 kV. The stereo-anaglyph was prepared from an image pair at ± 10° by using the Photoshop, which should be observed by the red and green stereo glasses.

Data analysis

The data are presented as means ± SE. Statistical significance was evaluated using the Student's *t*-test. All of the experiments were repeated at least three times.

Supplementary information for this article is available online: http://emboj.embopress.org

Acknowledgements

We gratefully thank T. Kirchhausen (Harvard University) for providing BS-C-1 cells expressing AP-2 σ2-GFP or LCa-GFP, J. C. Norman (Beatson Institute) for

instructing us in the analytic method for integrin endocytosis, K. Kato (Nagoya University) for providing the AP-2 construct, K. Ushida (Nagoya University) for capturing the transmission electron microscopic images, T. Fujimoto (Nagoya University) for helpful discussions on electron microscopy, and I. Mizuguchi (Nagoya University) for support in capturing images using the TIRF microscope. This work was supported by a Grant-in-Aid for Scientific Research (A) and (S), Grant-in-Aid for Scientific Research on Innovative Areas (to MT), Grant-in-Aid for Young Scientists (A) (to AE), Grant-in-Aid for Scientific Research (B) (23310087, 26286027 to NM), and Grant-in-Aid for Scientific Research (C) (25430118 to HM) commissioned by the Ministry of Education, Culture, Sports, Science and Technology of Japan, the Takeda Foundation (to AE), the Nakajima Foundation (to AE), and the Shimabara Science Promotion Foundation (to AE).

Author contributions

LW performed most of the experiments and analyzed the data. HM, KT, and HN assisted with dynamin GTPase assay. NA performed electron microscopy. NM performed freeze-replica electron microscopy. HM, KeKu, and TW assisted with the purification of recombinant proteins. PJ, JA, TK, MA, MI-T, and YM assisted with the experiments. KoKa was involved in study design. LW, AE, and MT designed the study and wrote the paper. MT provided team leadership and project management.

Conflict of interest

The authors declare that they have no conflict of interest.

References

Balklava Z, Pant S, Fares H, Grant BD (2007) Genome-wide analysis identifies a general requirement for polarity proteins in endocytic traffic. *Nat Cell Biol* 9: 1066 – 1073

Barylko B, Binns D, Lin KM, Atkinson MA, Jameson DM, Yin HL, Albanesi JP (1998) Synergistic activation of dynamin GTPase by Grb2 and phosphoinositides. *J Biol Chem* 273: 3791 – 3797

Borner GH, Harbour M, Hester S, Lilley KS, Robinson MS (2006) Comparative proteomics of clathrin-coated vesicles. *J Cell Biol* 175: 571 – 578

Borner GH, Antrobus R, Hirst J, Bhumbra GS, Kozik P, Jackson LP, Sahlender DA, Robinson MS (2012) Multivariate proteomic profiling identifies novel accessory proteins of coated vesicles. *J Cell Biol* 197: 141 – 160

Chappie JS, Mears JA, Fang S, Leonard M, Schmid SL, Milligan RA, Hinshaw JE, Dyda F (2011) A pseudoatomic model of the dynamin polymer identifies a hydrolysis-dependent powerstroke. *Cell* 147: 209 – 222

Collinet C, Stöter M, Bradshaw CR, Samusik N, Rink JC, Kenski D, Habermann B, Buchholz F, Henschel R, Mueller MS, Nagel WE, Fava E, Kalaidzidis Y, Zerial M (2010) Systems survey of endocytosis by multiparametric image analysis. *Nature* 464: 243 – 249

Damke H, Binns DD, Ueda H, Schmid SL, Baba T (2001) Dynamin GTPase domain mutants block endocytic vesicle formation at morphologically distinct stages. *Mol Biol Cell* 12: 2578 – 2589

Doherty GJ, McMahon HT (2009) Mechanisms of endocytosis. *Annu Rev Biochem* 78: 857 – 902

Ehrlich M, Boll W, Van Oijen A, Hariharan R, Chandran K, Nibert ML, Kirchhausen T (2004) Endocytosis by random initiation and stabilization of clathrin-coated pits. *Cell* 118: 591 – 605

Enomoto A, Murakami H, Asai N, Morone N, Watanabe T, Kawai K, Murakumo Y, Usukura J, Kaibuchi K, Takahashi M (2005) Akt PKB regulates actin organization and cell motility via Girdin APE. *Dev Cell* 9: 389 – 402

Enomoto A, Asai N, Namba T, Wang Y, Kato T, Tanaka M, Tatsumi H, Taya S, Tsuboi D, Kuroda K, Kaneko N, Sawamoto K, Miyamoto R, Jijiwa M, Murakumo Y, Sokabe M, Seki T, Kaibuchi K, Takahashi M (2009) Roles of disrupted-in-schizophrenia 1-interacting protein girdin in postnatal development of the dentate gyrus. *Neuron* 63: 774 – 787

Ezratty EJ, Bertaux C, Marcantonio EE, Gundersen GG (2009) Clathrin mediates integrin endocytosis for focal adhesion disassembly in migrating cells. *J Cell Biol* 187: 733 – 747

Faelber K, Posor Y, Gao S, Held M, Roske Y, Schulze D, Haucke V, Noé F, Daumke O (2011) Crystal structure of nucleotide-free dynamin. *Nature* 477: 556 – 560

Ferguson SM, Raimondi A, Paradise S, Shen H, Mesaki K, Ferguson A, Destaing O, Ko G, Takasaki J, Cremona O, O'Toole E, De Camilli P (2009) Coordinated actions of actin and BAR proteins upstream of dynamin at endocytic clathrin-coated pits. *Dev Cell* 17: 811 – 822

Ferguson SM, De Camilli P (2012) Dynamin, a membrane-remodeling GTPase. *Nat Rev Mol Cell Biol* 13: 75 – 88

Ghosh P, Beas AO, Bornheimer SJ, Garcia-Marcos M, Forry EP, Johannson C, Ear J, Jung BH, Cabrera B, Carethers JM, Farquhar MG (2010) A G{alpha} i-GIV molecular complex binds epidermal growth factor receptor and determines whether cells migrate or proliferate. *Mol Biol Cell* 21: 2338 – 2354

Gout I, Dhand R, Hiles ID, Fry MJ, Panayotou G, Das P, Truong O, Totty NF, Hsuan J, Booker GW, Campbell ID, Waterfield MD (1993) The GTPase dynamin binds to and is activated by a subset of SH3 domains. *Cell* 75: 25 – 36

Henry AG, Hislop JN, Grove J, Thorn K, Marsh M, von Zastrow M (2012) Regulation of endocytic clathrin dynamics by cargo ubiquitination. *Dev Cell* 23: 519 – 532

Huang F, Goh LK, Sorkin A (2007) EGF receptor ubiquitination is not necessary for its internalization. *Proc Natl Acad Sci USA* 104: 16904 – 16909

Jiang P, Enomoto A, Jijiwa M, Kato T, Hasegawa T, Ishida M, Sato T, Asai N, Murakumo Y, Takahashi M (2008) An actin-binding protein Girdin regulates the motility of breast cancer cells. *Cancer Res* 68: 1310 – 1318

Kaksonen M, Toret CP, Drubin DG (2006) Harnessing actin dynamics for clathrin-mediated endocytosis. *Nat Rev Mol Cell Biol* 7: 404 – 414

Keyel PA, Mishra SK, Roth R, Heuser JE, Watkins SC, Traub LM (2006) A single common portal for clathrin-mediated endocytosis of distinct cargo governed by cargo-selective adaptors. *Mol Biol Cell* 17: 4300 – 4317

Kitamura T, Asai N, Enomoto A, Maeda K, Kato T, Ishida M, Jiang P, Watanabe T, Usukura J, Kondo T, Costantini F, Murohara T, Takahashi M (2008) Regulation of VEGF-mediated angiogenesis by the Akt PKB substrate Girdin. *Nat Cell Biol* 10: 329 – 337

Kozik P, Hodson NA, Sahlender DA, Simecek N, Soromani C, Wu J, Collinson LM, Robinson MS (2013) A human genome-wide screen for regulators of clathrin-coated vesicle formation reveals an unexpected role for the V-ATPase. *Nat Cell Biol* 15: 50 – 60

Lakadamyali M, Rust MJ, Zhuang XW (2006) Ligands for clathrin-mediated endocytosis are differentially sorted into distinct populations of early endosomes. *Cell* 124: 997 – 1009

Lee CS, Kim IS, Park JB, Lee MN, Lee HY, Suh PG, Ryu SH (2006) The phox homology domain of phospholipase D activates dynamin GTPase activity and accelerates EGFR endocytosis. *Nat Cell Biol* 8: 477 – 484

Le-Niculescu H, Niesman I, Fischer T, DeVries L, Farquhar MG (2005) Identification and characterization of GIV, a novel G alpha i/s-interacting protein found on COPI, endoplasmic reticulum-Golgi transport vesicles. *J Biol Chem* 280: 22012 – 22020

Leonard D, Hayakawa A, Lawe D, Lambright D, Bellve KD, Standley C, Lifshitz LM, Fogarty KE, Corvera S (2008) Sorting of EGF and transferrin at the plasma membrane and by cargo-specific signaling to EEA1- enriched endosomes. *J Cell Sci* 121: 3445 – 3458

Levayer R, Pelissier-Monier A, Lecuit T (2011) Spatial regulation of Dia and Myosin-II by RhoGEF2 controls initiation of E-cadherin endocytosis during epithelial morphogenesis. *Nat Cell Biol* 13: 529 – 540

Liu AP, Aguet F, Danuser G, Schmid SL (2010) Local clustering of transferrin receptors promotes clathrin-coated pit initiation. *J Cell Biol* 191: 1381 – 1393

Loerke D, Mettlen M, Yarar D, Jaqaman K, Jaqaman H, Danuser G, Schmid SL (2009) Cargo and dynamin regulate clathrin-coated pit maturation. *PLoS Biol* 7: e57

Marchese A, Paing MM, Temple BR, Trejo J (2008) G protein-coupled receptor sorting to endosomes and lysosomes. *Annu Rev Pharmacol Toxicol* 48: 601 – 629

Martinu L, Santiago-Walker A, Qi H, Chou MM (2002) Endocytosis of epidermal growth factor receptor regulated by Grb2-mediated recruitment of the Rab5 GTPase-activating protein RN-tre. *J Biol Chem* 277: 50996 – 51002

McMahon HT, Boucrot E (2011) Molecular mechanism and physiological functions of clathrin-mediated endocytosis. *Nat Rev Mol Cell Biol* 12: 517 – 533

Mettlen M, Loerke D, Yarar D, Danuser G, Schmid SL (2010) Cargo- and adaptor-specific mechanisms regulate clathrin-mediated endocytosis. *J Cell Biol* 188: 919 – 933

Miaczynska M, Christoforidis S, Giner A, Shevchenko A, Uttenweiler-Joseph S, Habermann B, Wilm M, Parton RG, Zerial M (2004) APPL proteins link Rab5 to nuclear signal transduction via an endosomal compartment. *Cell* 116: 445 – 456

Nishimura T, Kaibuchi K (2007) Numb controls integrin endocytosis for directional cell migration with aPKC and PAR-3. *Dev Cell* 13: 15 – 28

Ohara K, Enomoto A, Kato T, Hashimoto T, Isotani-Sakakibara M, Asai N, Ishida-Takagishi M, Weng L, Nakayama M, Watanabe T, Kato K, Kaibuchi K, Murakumo Y, Hirooka Y, Goto H, Takahashi M (2012) Involvement of Girdin in the determination of cell polarity during cell migration. *PLoS ONE* 7: e36681

Padrón D, Tall RD, Roth MG (2006) Phospholipase D2 is required for efficient endocytic recycling of transferrin receptors. *Mol Biol Cell* 17: 598 – 606

Paterson AD, Parton RG, Ferguson C, Stow JL, Yap AS (2003) Characterization of E-cadherin endocytosis in isolated MCF-7 and Chinese hamster ovary cells: the initial fate of unbound E-cadherin. *J Biol Chem* 278: 21050 – 21057

Quan A, Robinson PJ (2005) Rapid purification of native dynamin I and colorimetric GTPase assay. *Methods Enzymol* 404: 556 – 569

Sato K, Watanabe T, Wang S, Kakeno M, Matsuzawa K, Matsui T, Yokoi K, Murase K, Sugiyama I, Ozawa M, Kaibuchi K (2011) Numb controls E-cadherin endocytosis through p120 catenin with aPKC. *Mol Biol Cell* 22: 3103 – 3119

Schmid SL, Frolov VA (2011) Dynamin- functional design of a membrane fission catalyst. *Annu Rev Cell Dev Biol* 27: 79 – 105

Sigismund S, Argenzio E, Tosoni D, Cavallaro E, Polo S, Di Fiore PP (2008) Clathrin-mediated internalization is essential for sustained EGFR signaling but dispensable for degradation. *Dev Cell* 15: 209 – 219

Simpson F, Martin S, Evans TM, Kerr M, James DE, Parton RG, Teasdale RD, Wicking C (2005) Novel hook-related protein family and the characterization of hook-related protein 1. *Traffic* 6: 442 – 458

Soulet F, Yarar D, Leonard M, Schmid SL (2005) SNX9 regulates dynamin assembly and is required for efficient clathrin-mediated endocytosis. *Mol Biol Cell* 16: 2058 – 2067

Takahashi K, Miyoshi H, Otomo M, Osada K, Yamaguchi N, Nakashima H (2010) Suppression of dynamin GTPase activity by sertraline leads to inhibition of dynamin-dependent endocytosis. *Biochem Biophys Res Commun* 391: 382 – 387

Tosoni D, Puri C, Confalonieri S, Salcini AE, De Camilli P, Tacchetti C, Di Fiore PP (2005) TTP specifically regulates the internalization of the transferrin receptor. *Cell* 123: 875 – 888

Traub LM (2009) Tickets to ride- selecting cargo for clathrin-regulated internalization. *Nat Rev Mol Cell Biol* 10: 583 – 596

Wirtz-Peitz F, Zallen JA (2009) Junctional trafficking and epithelial morphogenesis. *Curr Opin Genet Dev* 19: 350 – 356

Zoncu R, Perera RM, Balkin DM, Pirruccello M, Toomre D, De Camilli P (2009) A phosphoinositide switch controls the maturation and signaling properties of APPL endosomes. *Cell* 136: 1110 – 1121